Available online at www.sciencedirect.com

ScienceDirect

Advances in Space Research 59 (2017) 2019–2031

ADVANCES IN SPACE RESEARCH (a COSPAR publication)

www.elsevier.com/locate/asr

Unsupervised change detection in a particular vegetation land cover type using spectral angle mapper

Diego Renza [a,*], Estibaliz Martinez [b], Iñigo Molina [b], Dora M. Ballesteros L. [a]

[a] Universidad Militar Nueva Granada, Bogotá, Colombia
[b] Universidad Politécnica de Madrid, Madrid, Spain

Received 9 August 2016; received in revised form 15 December 2016; accepted 17 January 2017
Available online 3 February 2017

Abstract

This paper presents a new unsupervised change detection methodology for multispectral images applied to specific land covers. The proposed method involves comparing each image against a reference spectrum, where the reference spectrum is obtained from the spectral signature of the type of coverage you want to detect. In this case the method has been tested using multispectral images (SPOT5) of the community of Madrid (Spain), and multispectral images (Quickbird) of an area over Indonesia that was impacted by the December 26, 2004 tsunami; here, the tests have focused on the detection of changes in vegetation. The image comparison is obtained by applying Spectral Angle Mapper between the reference spectrum and each multitemporal image. Then, a threshold to produce a single image of change is applied, which corresponds to the vegetation zones. The results for each multitemporal image are combined through an exclusive or (XOR) operation that selects vegetation zones that have changed over time. Finally, the derived results were compared against a supervised method based on classification with the Support Vector Machine. Furthermore, the NDVI-differencing and the Spectral Angle Mapper techniques were selected as unsupervised methods for comparison purposes. The main novelty of the method consists in the detection of changes in a specific land cover type (vegetation), therefore, for comparison purposes, the best scenario is to compare it with methods that aim to detect changes in a specific land cover type (vegetation). This is the main reason to select NDVI-based method and the post-classification method (SVM implemented in a standard software tool). To evaluate the improvements using a reference spectrum vector, the results are compared with the basic-SAM method. In SPOT5 image, the overall accuracy was 99.36% and the κ index was 90.11%; in Quickbird image, the overall accuracy was 97.5% and the κ index was 82.16%. Finally, the precision results of the method are comparable to those of a supervised method, supported by low detection of false positives and false negatives, along with a high overall accuracy and a high kappa index. On the other hand, the execution times were comparable to those of unsupervised methods of low computational load.

Keywords: Spectral angle mapper; Change detection; Vegetation land cover; SPOT5; Quickbird

1. Introduction

Change detection (CD) is the process of identifying differences in the state of an object or phenomenon through observation at different times (Singh, 1989). In general, CD involves the application of multitemporal (MT) datasets to quantitatively analyze temporal effects of a phenomenon (Lu et al., 2004). Although change detection techniques in remote sensing have had a significant increase in the last three decades, there is still work to do, such as identify changes in a particular landcover (Tewkesbury et al., 2015; Weng et al., 2014).

* Corresponding author.
E-mail addresses: diego.renza@unimilitar.edu.co (D. Renza), emartinez@fi.upm.es (E. Martinez), inigo.molina@upm.es (I. Molina), dora.ballesteros@unimilitar.edu.co (D.M. Ballesteros L.).

http://dx.doi.org/10.1016/j.asr.2017.01.027
0273-1177/

Generally, in a CD project, three main stages can be identified: (1) pre-processing, (2) selection of appropriate techniques to implement the analysis of CD, and (3) accuracy assessment of the results. Additionally, there are four important components to consider with regard to this process: pre-processing of input images, defining the unit of analysis, selecting a comparison method, and obtaining the change map for interpretation and accuracy assessment (Lu et al., 2004).

Regarding the unit of analysis, techniques can be grouped in seven categories, namely: pixel, kernel, image-object overlay, image-object comparison, multi-temporal image-object, vector polygon and hybrid schemes. Considering comparison methods, there are six categories to group them: layer arithmetic, post-classification change, direct classification, transformation, change vector analysis and hybrid change detection. Of these, the pixel and post-classification categories remain the most popular choices (Tewkesbury et al., 2015).

In post-classification change approaches, and in general, in supervised methods, a common resource is to exploit all available spectral channels due to the descriptive nature of the results allowing specific thematic questions to be answered (Tewkesbury et al., 2015). The aim of these methods is to generate a CD map, where modified and transition classes in land cover can be identified, i.e. it highlights specifically what has changed. Here, the changes are detected and labeled through supervised classification schemes; therefore, post-classification comparison is a suitable method to implement when sufficient training sample data are available (Lu et al., 2004). Thus, in some of these methods, ground truth information is required. However, in most practical cases, that information is not available or it is not easy to obtain (Bovolo et al., 2012).

If ground truth information is not available, there are unsupervised methods that produce a binary CD map in which change areas are distinguished from unchanged areas, i.e. relative change detection shows that something has changed but does not specify what that change is; i.e. they are not able to properly detect the presence of multiple changes in an unsupervised and automatic way (Bovolo et al., 2012; Lu et al., 2004). On the other hand, their main advantage is to provide a faster method for quickly comparing images.

In recent years, kernel-based methods have shown high accuracy in unsupervised change detection problems. In Kernel-based methods, the non-linear decision function is generally obtained by running a linear algorithm in a higher dimensional feature space (Shah-Hosseini et al., 2015b; Shah-Hosseini et al., 2015a), i.e. the concept of the difference image, common to many change-detection methods, is extended to higher dimensional feature spaces (Volpi et al., 2012).

Recently, a broad group of kernel-based methods have been proposed. In Shah-Hosseini et al. (2015b), a similarity space based on few labeled training samples in high dimensional spaces was used to propose a hybrid kernel-based change detection method. In another work (Bovolo et al., 2010), the change detection problem is formulated in a high dimensional Hilbert space, and it is treated as a minimum enclosing ball problem, solving it by means of support vector domain description. The approach showed in Bovolo et al. (2007), combines the CVA (Change Vector Analysis) technique with a semi-supervised SVM classifier, exploiting a pseudo-training set and the original images to obtain the change detection map. In Shah-Hosseini et al. (2015a), two approaches for automatic CD framework are presented: the first method is based on the integration of CVA method, kernel-based C-means clustering, and kernel-based minimum distance classifier; in addition, a SVM-based CD method is presented and analyzed. One more non-linear approach is proposed in Volpi et al. (2010); here, an initialization routine is used in conjunction with an unsupervised cost function to optimize the kernel hyper parameters.

There are some aspects to consider when using kernel-based CD approaches. These aspects have to do with the fact that non-automatic kernel-based methods require labeled samples for training a classifier (Shah-Hosseini et al., 2015b), otherwise optimal kernel parameters and precise training samples have to be defined (Volpi et al., 2010; Shah-Hosseini et al., 2015a); therefore, some of these methods could be inefficient as far as run time is concerned (Shah-Hosseini et al., 2015b). For instance, in all the tests presented in Bovolo et al. (2010), the initialization threshold value was obtained according to a manual-trial-and-error procedure; moreover, in order to reduce the computational load of the training stage, the resulting sets were randomly sub-sampled. Furthermore, the output in kernel-based methods detects changes of any kind.

In conclusion, the complexity and the computational load of the kernel-based methods can be a disadvantage related to the simplicity of methods that reduce the CD problem to a 1-D problem by considering only the magnitude of the spectral change vectors (Bovolo et al., 2012). In the latter case, unsupervised CD procedures that use a single band are easy to apply and interpret, since a simple thresholding operation is required to obtain a change/no-change map (Bovolo et al., 2012). Its challenge is to find an algorithm that includes the different results of all bands so they can be integrated in a single result. For example, if an algorithm makes a comparison of each band for two MT images (n-bands), n difference images are obtained. Hence, it is necessary to apply n thresholds obtaining n change masks. Subsequently, it is necessary to define a methodology that integrates the n results; this methodology can be a mathematical operation, such as a normalized difference (integrates two bands) or spectral-quality indices that take into account all n bands in the comparison process. Consequently, the simultaneous use of multiple bands can produce better results (Im et al., 2007), since the multi-band problem is reduced to a 1-D problem by considering only the magnitude of spectral change vectors (Bovolo et al., 2012).

Some approaches suggest using spectral similarity metrics in order to integrate multiple bands in a CD process, as presented in previous work (Renza et al., 2013), which was aimed at detecting general changes, i.e. for any land cover class. However, in some cases it may be beneficial to detect different kinds of changes, for example changes in vegetation, water bodies, urban land, etc. (Bovolo et al., 2012). In spite of this, some other methods allow discrimination between selected land cover classes (Wang et al., 2009). For example, this is the case for methods based on Normalized Difference Vegetation Index (NDVI) differencing, which provides specific changes in vegetation (Teng et al., 2008). In this respect, where spectral similarities are required to identify different land cover change classes, spectral angular distances can be a useful solution, however, when using spectral similarity metrics, they can consider all available spectral bands, thus avoiding the need of prior information about relevant features (Bovolo et al., 2012). Nevertheless, the problem to properly detect the presence of different kinds of changes persists.

In this sense, the objective of this paper is to propose an unsupervised CD methodology with the following characteristics: the use of multiband images reducing the problem to a 1-D problem, low computational load, and it is a generic approach to detect a specific kind of change (vegetation). The proposed unsupervised CD methodology uses a spectral similarity metric, which can serve to detect the required kind of change (vegetation). The proposed approach uses the Spectral Angle Mapper (SAM) between a reference spectrum and each of the MT images, where the reference spectrum is defined according to the typical spectral signature of vegetation. SAM comparisons are binarized using a threshold and then combined through a logical operation.

2. Proposed CD method

In this section the proposed unsupervised CD approach is described. The unit of analysis is the pixel, whereas the comparison method is SAM-based using both MT images and a reference spectrum; furthermore, for obtaining a change/no change map a thresholding is used. The whole process consists of the following operations: pre-processing, reference spectrum, comparison, thresholding and combination, and evaluation. A general scheme of the proposed method is shown in Fig. 1.

2.1. Pre-processing

In this first phase, applying correction or using corrected data is a requirement for quantitative analysis of MT images. Therefore, the two MT images have to be radiometrically and atmospherically corrected and co-registered (Bovolo et al., 2012). One important thing to keep in mind, if it is possible, is to use data from the same sensor and to acquire it at the same time of the year (Lu et al., 2004).

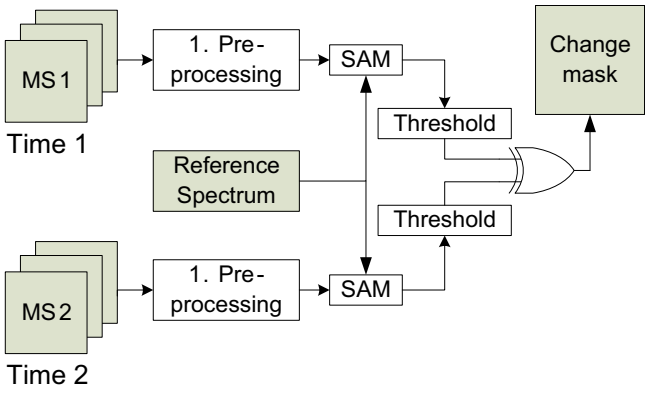

Fig. 1. Illustrative representation of the flow chart for change detection with SAM index.

According to the above, two MS images of SPOT5 sensor with a spatial resolution of 10 m and 1024 × 1024 pixels were selected. They correspond to 2005 and 2008 and were captured in the same month (June) in order to minimize the effect of solar lighting and seasonal differences. These images were registered in ENVI Software using 89 tie points, a first order polynomial function and bilinear resampling; a RMS Error of 0.556519 was obtained. The zone comprises parts of the Community of Madrid (Spain) and both show a high proportion of changes in vegetation covers. In this case, the bands of the visible spectrum (G, R) and Near-Infrared (NIR) of the SPOT5 MS images were used. The false color composition (NIR-R-G) for the two MT images are shown in Fig. 2.

Also, two MS images of Quickbird sensor with a spatial resolution of 2.5 m and 1500 × 1500 pixels were selected. They correspond to April, 2004 and January, 2005. The images correspond to an area over Indonesia that was impacted by the December 26, 2004 tsunami, where many vegetation areas were washed out by the tsunami. The images are publicly available through the ENVI tutorials on the following link http://exelis.http.internapcdn.net/exelis/data/ENVITutorialData.zip. In this case, the bands of the visible spectrum (B, G, R) and Near-Infrared (NIR) of the Quickbird MS images were used. The true color composition (R-G-B) for the two MT images are shown in Fig. 3.

2.2. Obtaining reference spectrum

The reference vector is defined based on the variation of reflectance with wavelength, i.e. the spectral reflectance for a particular land cover. The spectral reflectance is the ratio of reflected energy to incident energy as a function of wavelength. Also, the average of the values of spectral-reflectance over well defined wavelength bands, make up the spectral signature of a terrain feature by which it can be distinguished (Rees and Rees, 2013; Aggarwal, 2004). Fig. 4 illustrates schematically the spectral reflectance of four materials, in the wavelength range from 0.4 to

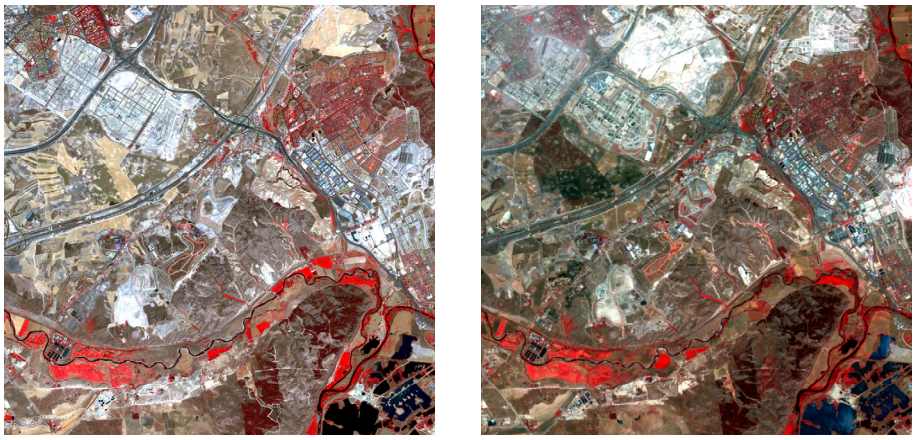

(a) Image of 2005. (b) Image of 2008.

(c)

Fig. 2. SPOT5 Multitemporal images used. 1024 × 1024 pixels false color NIR, red and green composition. The upper left corner is placed at 446404.73 E and 4470730.4 N (UTM geographic coordinates, zone 30, WGS-84). (For interpretation of the references to color in this figure legend, the reader is referred to the web version of this article.)

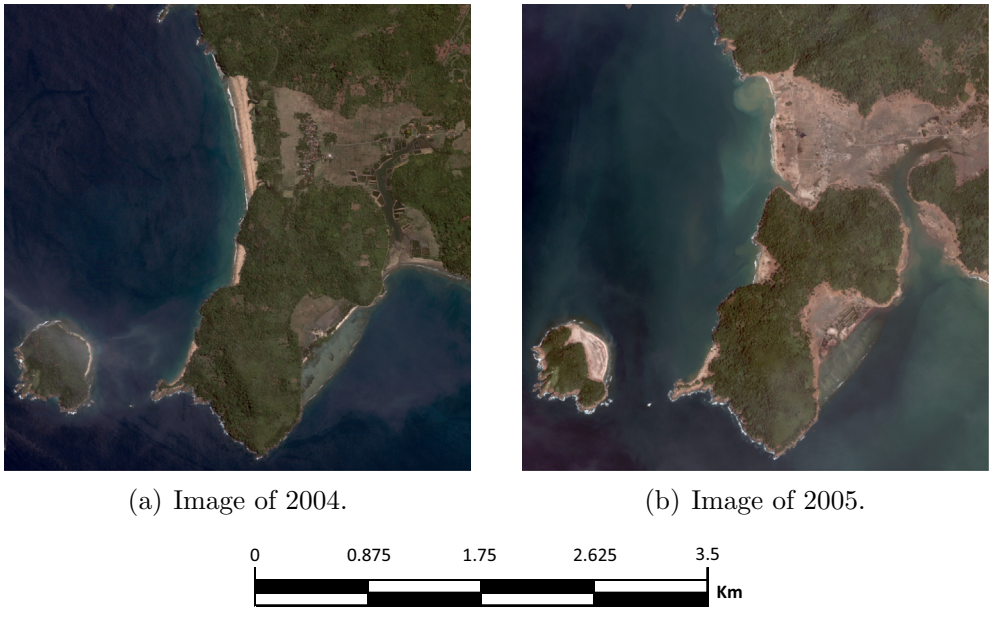

(a) Image of 2004. (b) Image of 2005.

(c)

Fig. 3. Quickbird Multitemporal images used. 1500 × 1500 pixels true color composition. The upper left corner is placed at 743959.221 E and 586709.556 N (UTM geographic coordinates, zone 46 N, WGS-84). (For interpretation of the references to color in this figure legend, the reader is referred to the web version of this article.)

1.05 μm, highlighting the G, R and NIR spectral bands. Here, it should be noted that the shape of such a curve represents the characteristic of the material and so allows to identifying it. The spectral signatures of water in Fig. 4 show that the most of longer visible wavelengths and the NIR radiation is absorbed or transmitted, i.e. it is not reflected. In the spectral signature of soil it should be noted that the most of radiation is either reflected or absorbed. The distinctive spectral signature of vegetation is characterized by a low reflectance in the visible region because of the presence of pigments, such as chlorophyll; also it is characterized by a scattering effect in the NIR, i.e. a high reflectance roughly between 0.7 and 1.3 μm (Rees and Rees, 2013; Aggarwal, 2004).

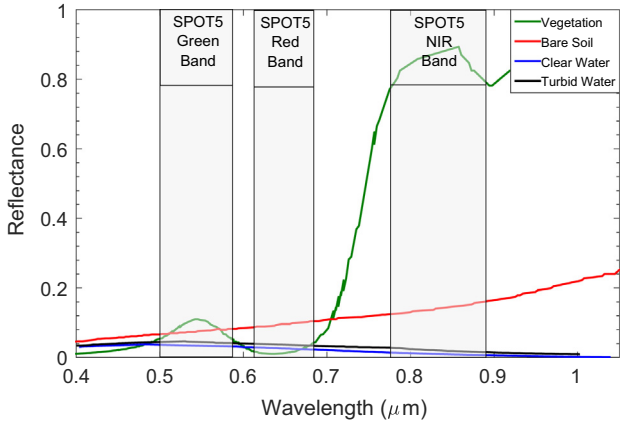

Fig. 4. Typical spectral reflectances of vegetation, soil and water in the visible and NIR regions (schematic) (Rees and Rees, 2013; Aggarwal, 2004).

According to the above, the typical spectral signature of healthy vegetation in MS images (SPOT5 and Qickbird) will be used to obtain the reference vector (Fig. 4). Using these images, the spectral signature of healthy vegetation (from highest to lowest) correspond to NIR, Green, Blue and Red bands. According to Fig. 4, their average reflectance ($\overline{R}$) values are equal to $\overline{R}_{NIR} = 0.88$, $\overline{R}_{Green} = 0.12$, $\overline{B}_{Green} = 0.06$ and $\overline{R}_{Red} = 0.03$. To normalize data, each of these values is divided by the sum of all factors and multiplied by $2^{nbits-1}$ (Eq. (1)) (where *nbits* is the radiometric resolution of the MS bands, i.e. the amount of bits used to represent each pixel).

$$W_i = 255 \times \frac{\overline{R}_i}{\sum_i^N R_i} \tag{1}$$

For $i = 1, 2, \ldots, N$, and N is the number of bands of the MS image. Finally, the reference vector (RV) is given by the Eq. (2).

$$RV = [\, W_1 \quad W_2 \quad \ldots \quad W_N \,] \tag{2}$$

2.3. Image comparison by means of SAM index

The core of the image comparison in the proposed method is a spectral angular distance (SAD). The SAD has previously been used as the metrics for classification and clustering of MS images (van der Meer, 2006). So, Spectral Angle Mapper (SAM) and Spectral Correlation Mapper (SCM) procedures may be two effective solutions for mapping these similarities. In Carvalho Júnior et al. (2011), these main correlation measures were used for unsupervised detection of multiple changes in multitemporal images; in that study case, the similarity measure that had the best performance was SAM, and therefore this is the spectral similarity metric selected in this paper to the proposed CD method. The SAM index measures the spectral similarity of an image against a reference spectrum by calculating the angle between them; both the image and the spectrum are treated as a vector in a space with dimensionality equal to the number of bands. On the other hand, SCM is a variant of $cos(SAM)$, however SCM standardizes the data, centralizing it in the mean of the two spectra; i.e. SCM is similar to Correlation Coefficient of Pearson (De Carvalho and Meneses, 2000; Carvalho Júnior et al., 2011).

According to the above, the basis of image comparison is an index of spectral similarity derived from multi-band images known as SAM. This method allows us to determine the degree of spectral similarity of an image against a reference spectrum. This similarity is expressed in terms of the average angle between the two spectra. At each absolute position k, the image spectrum will be a vector whose elements correspond with the pixel values at location k for each of the bands. That is, the two spectra are handled as vectors in space, whose dimension is equal to the number of bands (N); therefore, for each pixel the result is an angular difference measured in radians or degrees. Generally, these results can be averaged for the whole image, in order to obtain an overall measure of spectral distortion.

To obtain the difference images, the reference vector (Eq. (2)) is compared against each one of the image vectors of the two MT images. The image vector (IV) of each MT image is given by the Eq. (3).

$$IV_{MT_i}(k) = [\, DN_{1,k} \quad DN_{2,k} \quad \ldots \quad DN_{N,k} \,] \tag{3}$$

where $i = 1, 2$ corresponds to the index of each MT image. $k = 1, 2, \ldots, K$ is the absolute position of pixel $k - th$, being $K = X \times Y$, and X, Y the image dimensions. DN is the pixel value (Digital Number) at position k, and $n = 1, 2, \ldots, N$ is the index for each one of the MS bands.

The result of comparing the image vector of each MT image with the reference vector is a difference image (DI). Each pixel of the DI for each MT image is obtained as the absolute value of the spectral angle between the two vectors, Eq. (4).

$$DI_{MT_i}(k) = arccos\left(\frac{\langle RV(k), IV_{MT_i}(k)\rangle}{\|RV(k)\|_2 \cdot \|IV_{MT_i}(k)\|_2}\right) \tag{4}$$

where $\langle \cdot, \cdot \rangle$ represents scalar product and $\| \cdot \|$ denotes the L^2 norm (Euclidean norm or the ordinary distance from the origin to the point), and $i = 1, 2$ corresponds to the index of each MT image.

As previously discussed, the objective of SAM is to identify changes in spectral shape, being invariant to the gain or intensity values (often cited in remote sensing as a suppression of illumination effects). Its result is an angle value ranging from 0 to $\pi/2$, where zero is its ideal value, indicating the absence of spectral distortion, but not necessarily indicating intensity equality. In order to include measures for both spectral and intensity distortion, SAM can be used in conjunction with spectral measurements as ERGAS (in French "Erreur Relative Globale Adimensionnelle de Synthèse") (Renza et al., 2011). However, when images present intensity distortions, as in the case of satellite images, this SAM feature can result in an advantage. That

is, SAM index allows the comparison of spectral differences in two images, preventing their radiometric differences from becoming significant (Moughal and Yu, 2014).

It is important to note that the proposed method could detect changes including any number of bands of the original images. To add, regardless of the number of used bands, the image resulting from the comparison is a single band and it is the input to a thresholding process. Also, regarding the characteristics of the bands, these can be selected according to the type of CD you wish to prioritize, i.e. the angle between two spectra can increase or decrease depending on the bands submitted to it. This is particularly important in hyperspectral images; therefore, some approaches have been proposed to select bands that increase the angle between two spectra (Keshava, 2004).

2.4. Thresholding and combination

In the previous step, each image is compared against the reference vector. The result is a gray-scale image (DI_{MT_i}) that has to be thresholded to discriminate between change areas and non-change areas. In this work, the selected thresholding technique for the proposed scheme is the Kapur technique (Kapur et al., 1985), because of it has shown one of the best performances for change detection (Rosin and Ioannidis, 2003; Sahoo et al., 1988; Sezgin and Sankur, 2004; Rosin, 1998). Then a binary image (BI) is obtained by applying a threshold in each one of the MT images.

$$BI_{MT_i} = th(DI_{MT_i}) \tag{5}$$

where $th()$ is the thresholding function given by the Kapur technique. In the compared methods (NDVI differencing and basic-SAM methods), in addition to the Kapur method, Otsu (1975) and Tsai (1985) thresholding techniques are evaluated.

The binary images obtained after thresholding each MT image, discriminate between vegetation and non-vegetation zones. These binary images are combined through selection of the pixels where there is no coincidence in vegetation zones, i.e. where there are changes. This phase is made by means of an XOR operation; therefore, finally the change mask is obtained through the Eq. (6).

$$CM = BI_{MS_1} \oplus BI_{MS_1} \tag{6}$$

2.5. Evaluation

To assess the accuracy of a classification method, one of the most used approaches is the error matrix evaluation method (Foody, 2002). In order to determine the accuracy of CD analysis, error matrices are constructed by comparing the obtained results against change supervised areas. Then, Overall Accuracy (OA) and Kappa (κ) indices are calculated to evaluate the binary change image (Lu and Weng, 2007). OA is the sum of the pixels correctly classified divided by the total number of reference pixels, while κ index is a statistical measure of coincidence between two maps, in this case, between the output classification change/non-change map and the reference map.

Being FP the false positives, FN the false negatives, TP the true positives, TN the true negatives, and $T = FP + FN + TP + TN$. False positives are the unchanged pixels erroneously categorized as changed pixels; false negatives are changed pixels categorized erroneously as unchanged pixels; true positives are changed pixels correctly categorized and true negatives are unchanged pixels correctly categorized. Finally, OA is calculated, as follows (Eq. (7)):

$$OA = \frac{TP + TN}{TP + TN + FP + FN} \tag{7}$$

And the kappa index is obtained according to the Eq. (8):

$$\kappa = \frac{OA - P_e}{1 - P_e} \tag{8}$$

where P_e is defined as in Eq. (9):

$$P_e = \{P_1 \times P_2\} + \{(1 - P_1) \times (1 - P_2)\} \tag{9}$$

where P_1 is the number of pixels categorized as changed, divided by the total number of pixels of the image (i.e. $P_1 = (TP + FP)/T)$). P_2 is the real number of changed pixels divided by the total number of pixels (i.e. $P_2 = (TP + FN)/T)$).

OA ranges from 0 to 1, being this last the ideal value (i.e. all changed and unchanged pixels are correctly classified). The kappa index ranges from -1 to 1, where -1 means perfect and consistent disagreement, 1 means perfect agreement, and 0 means a random level of agreement/disagreement (Srivastava et al., 2012).

Finally, a detailed scheme of the proposed method is depicted in Fig. 5.

3. Implementation and evaluation of the method

3.1. Change detection algorithms

Since the proposed method is unsupervised, it would be feasible to compare the results against a supervised method. In this case, a classification-based method (Support Vector Machine, SVM) was selected as the reference method (Srivastava et al., 2012). Besides, two well-known unsupervised methods were compared to SVM, too: NDVI differencing and basic-SAM (between MT images, i.e. without reference spectrum). It should be noted that these methods can be considered as unsupervised methods, since they do not require training data, and as long as an automatic thresholding technique is used. So, the following methods were implemented:

Method 1: SVM classification. For SVM supervised classification, the training areas were selected according to four thematic classes (buildings, water, soil and vegeta-

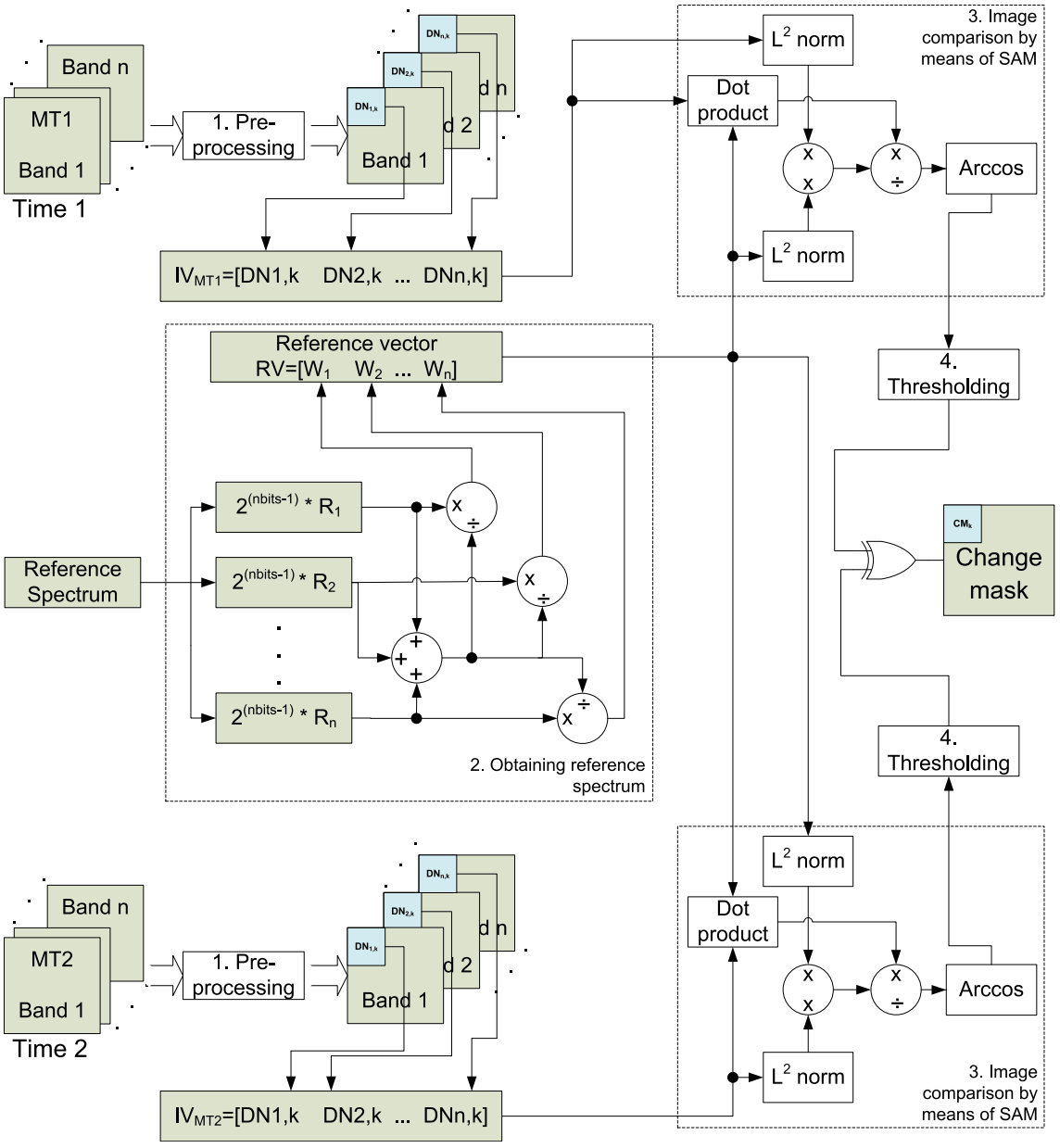

Fig. 5. Detailed representation of the flow chart for change detection with SAM index.

tion) derived through scatter diagram methodology (Martinez et al., 1999) and visual image inspection. In both MT images, the training areas were carefully selected in the same geographical location and the correspondence with the same class was verified. Next, the vegetation classes were extracted and their absolute difference was taken as an image of change.

Method 2: Proposed method. Through SAM, comparing each MT image against the reference spectrum using the method described above. Thresholding with Kapur method and then applying an XOR operation between the two masks.

Method 3: Basic-SAM (without reference spectrum). Apply SAM between the MT images and threshold with Kapur, Otsu or Tsai method obtaining a change/non-change mask.

Method 4: NDVI differencing. Apply NDVI in each MT image and obtain the absolute difference between the two NDVI components; thresholding with Kapur, Otsu or Tsai method.

For the evaluation process, the proposed method and the three additional methods mentioned above were applied to the two datasets. In each case, a binary mask indicating the changes was obtained. The masks resulting from the proposed method and the basic-SAM and the NDVI methods were compared against the mask obtained with the SVM-based method. Matrices errors were

obtained and quantitative assessments for the OA and κ indices were calculated.

3.2. Results and discussion

3.2.1. SPOT5 case

The difference images obtained by the evaluated comparison methods are shown in Fig. 6. The result of the comparison obtained with the proposed method (comparison of the reference spectrum against the image of 2005 and the image of 2008) are showed in Fig. 6(a) and (b) respectively; in these two figures it is clear that the vegetation zones can be easily discriminated (bright zones), allowing the integration of the two results (XOR operation). In the case of the difference images obtained with the basic-SAM method (Fig. 6(c)) and NDVI method (Fig. 6(d)), it is also possible to discriminate the vegetation zones; however, other types of coverage are showed as bright zones, particularly the water bodies in the lower right.

For quantitative evaluation, overall accuracy and kappa indices were obtained for the proposed method, the basic-SAM and the NDVI-based methods with respect to the post-classification method based on SVM (Table 1). In the last two cases the three thresholding methods discussed above are evaluated.

According to the results showed in Table 1, the OA and κ values for the proposed method are the highest because it has the greatest amount of true positives and the lowest number of false negatives. In the Basic-SAM and NDVI methods, it can be seen that they obtain a high value of OA, however their kappa index is low; this is mainly due to the OA only takes into account the pixels correctly classified (true positives and true negatives), whereas kappa index takes into account both the pixels correctly classified as the pixels misclassified (false negatives and false positives). When the results of the compared methods (Basic-SAM and NDVI) are analyzed, it should be noted that these have a high number of false negatives for all thresholding techniques; also they have a high number of false positives for all methods of thresholding, except for the Kapur method. The latter is mainly due to the high threshold value given by this technique, leading to a detection of few change zones.

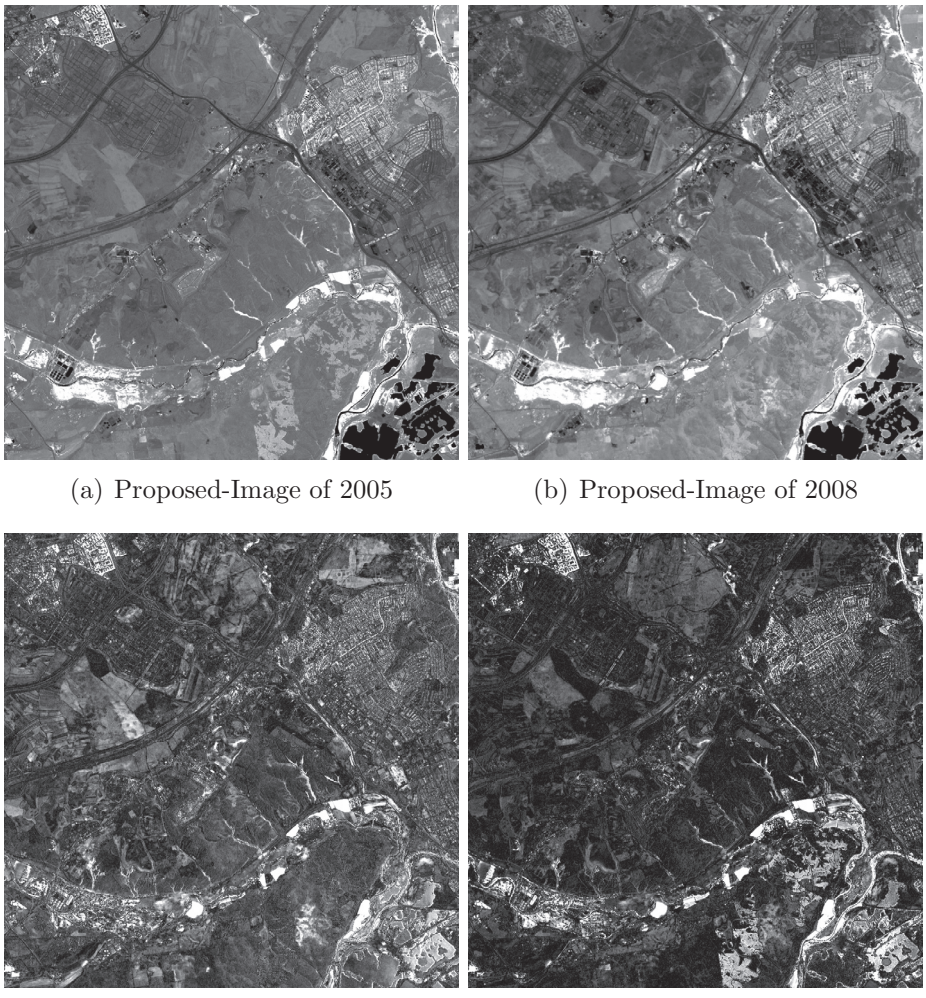

(a) Proposed-Image of 2005 (b) Proposed-Image of 2008

(c) Basic-SAM (d) NDVI

Fig. 6. SPOT 5 Case. Difference images (grayscale) obtained by the evaluated comparison methods.

Table 1
SPOT 5 Case. Classification accuracy results obtained for the unsupervised detection methods, through the comparison against a supervised method (SVM-based) (results are shown in percentages).

Comparison and thresholding method		C	NC	Total	OA (%)	κ (%)
Proposed	C	31535	3539	35074	99.36	90.11
	NC	3128	1010374	1013502		
Basic-SAM (Kapur)	C	8279	2453	10732	97.25	35.47
	NC	26384	1011460	1037844		
NDVI (Kapur)	C	9103	3975	13078	97.18	36.99
	NC	25560	1009938	1035498		
Basic-SAM (Otsu)	C	22785	53462	76247	93.77	38.28
	NC	11878	960451	972329		
NDVI (Otsu)	C	22661	57565	80226	93.37	36.52
	NC	12002	956348	968350		
Basic-SAM (Tsai)	C	20606	35242	55848	95.30	43.22
	NC	14057	978671	992728		
NDVI (Tsai)	C	20506	43087	63593	94.54	39.14
	NC	14157	970826	984983		
	Total	34663	1013913	1048576		

C: Change (pixels) and NC: No-change (pixels).

Fig. 7 corresponds to the mask of changes obtained through each of the four comparison methods mentioned above. Again, in Basic-SAM and NDVI, the thresholding with Kapur, Otsu and Tsai methods are evaluated. The change mask obtained with the proposed method (Fig. 7 (b)) are clearly very similar to the change mask obtained with the SVM-based method, agreeing with the results of Table 1. The important thing here is that only areas that correspond to vegetation are detected (e.g. no water bodies in the lower right are detected). To justify this result, it is necessary to observe the false color images of Fig. 2. As can be seen, there are no vegetation zones in any of the water bodies of these images, so the result of a change detection process in vegetation should not include these areas.

The change masks obtained with the basic-SAM method and NDVI method by using Kapur thresholding (Fig. 7(c), (f)) show a high number of false negatives, i.e. there are several vegetation zones that are no detected. In these schemes, since the difference image is dark, the lower the threshold value is, the higher the number of true positives; their problem is that by lowering the threshold value, the higher the amount of false positives. This can be seen as the detection of areas that do not correspond to vegetation appear (e.g. water bodies in the lower right). However, as discussed above, the spectral signature of healthy vegetation is far from the spectral signature of water. In the NDVI method, these areas are probably detected by the presence of underwater vegetation; in the case of basic-SAM, the simple spectral difference of the two areas is what originates its detection, i.e. it does not consider the spectral signature of the type of coverage to be detected. The above can be evidenced with masks obtained using the methods of Otsu and Tsai (Figs. 7(c), (d), (f), (g)).

3.2.2. Quickbird case

The proposed method was also tested on Quickbird images, evaluating the performance of the proposed method in natural disasters monitoring. For this purpose, the Blue, Green, Red and NIR bands were used. The reference spectrum was obtained according to Fig. 4, using the aforementioned bands. Regarding the thresholding technique, here the threshold value was obtained by means of balancing of false positive rate against the false negative rate; This was applied both in the proposed method and in the NDVI and SAM-based methods. This was done to test the systems in the best case possible, specifically as far as kappa index is concerned. In this way, the difference images obtained by the evaluated comparison methods are shown in Fig. 8. Here again the two comparison images obtained with the proposed method, allow to easily discriminate the vegetation zones, to later obtain the differences between them (Fig. 8(a) and (b)). In the case of the difference images obtained by the methods based on basic-SAM and NDVI (Fig. 8(c) and (d)), the bright areas are the zones of change, which will later be obtained through the thresholding process. In any case, the changes present in the evaluated images correspond, in great majority to changes in vegetation, reason why the results of these last two methods will improve with respect to the SPOT5 case.

Fig. 9 corresponds to the mask of changes obtained through each of the four methods mentioned above. The masks obtained by the evaluated methods are clearly very similar, there are, however slight variations between each mask. Particularly, the masks obtained with the SVM and the proposed methods show some small areas that are not present in the masks of the other two methods, which results in an increased number of true positives iden-

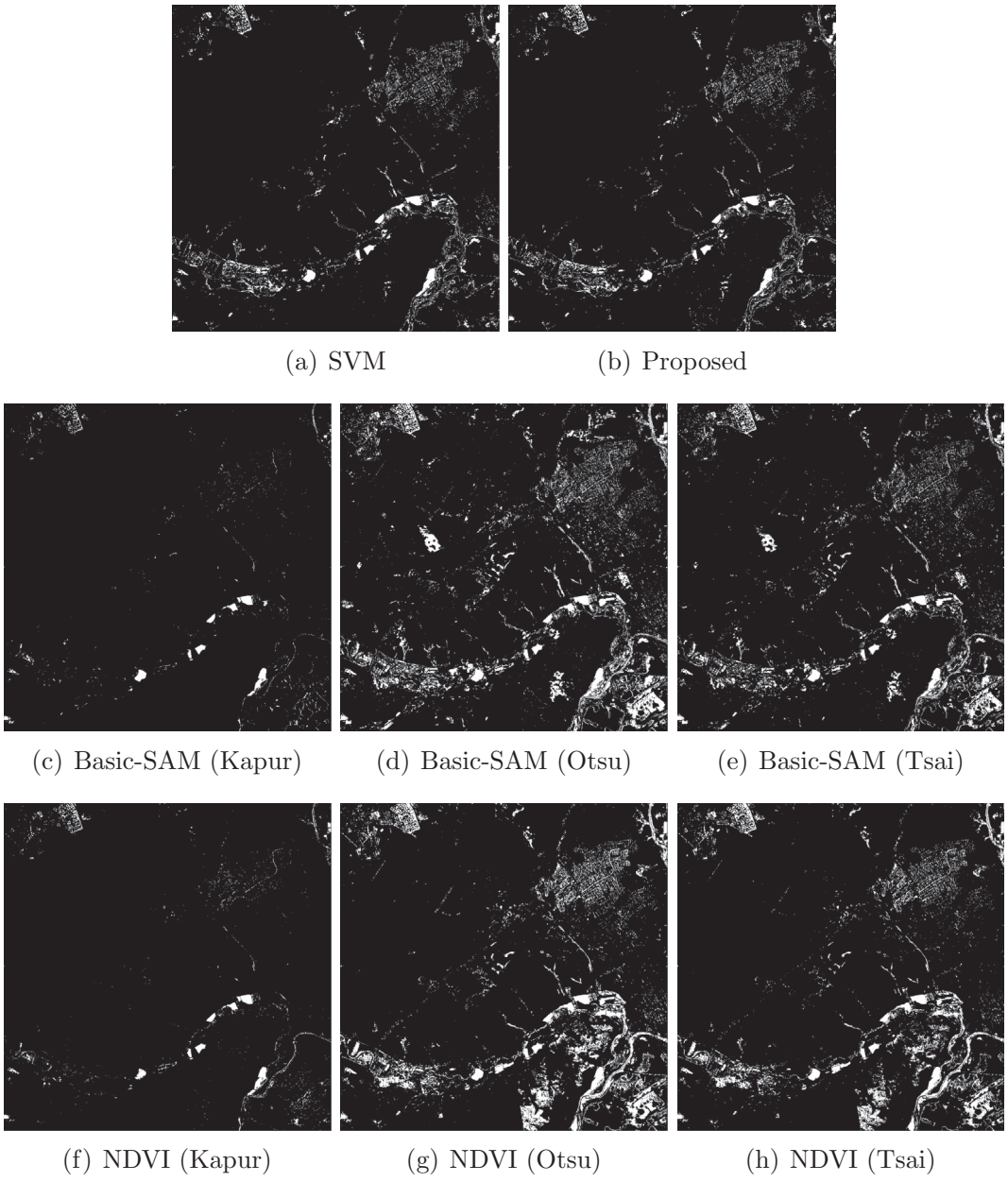

Fig. 7. SPOT 5 Case. CD masks obtained for the unsupervised detection methods and three different thresholding methods, through the comparison against a supervised method (SVM-based). Change areas in white and non-change areas in black.

tified in the proposed method, and therefore it also leads to an increased number of false negatives in the change masks obtained with the NDVI and SAM-based methods.

Table 2 shows the proportion of values obtained for false positives, true positives, false negatives and true negatives, and the corresponding overall accuracy and kappa indices. Here again, quantitative evaluation is made respect to the post-classification method based on SVM. It should be noted here that the proportion of data correctly identified (true positives and true negatives) by the proposed method is higher than that of the other two methods, while the zones incorrectly detected (false positives and false negatives) are lower. Although OA values are similar for all three methods, the k index shows a better result in the proposed method, since the number of pixels correctly classified is higher, whereas the number of misclassified pixels is lower, in respect to the two other methods.

3.2.3. Comparison in terms of computational load

In order to perform a comparative analysis regarding computational load, the execution time of the unsupervised detection algorithms was measured. The algorithms were run on Windows 8.1 (64-bit), with a 3.2 GHz Intel Core i7-4790S processor and 8 GB of RAM. The results are shown in Table 3.

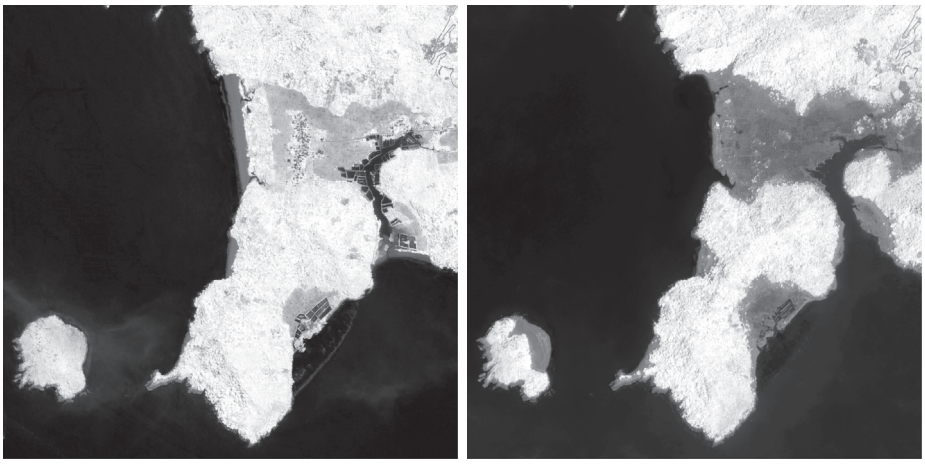

(a) Proposed-Image of 2005 (b) Proposed-Image of 2008

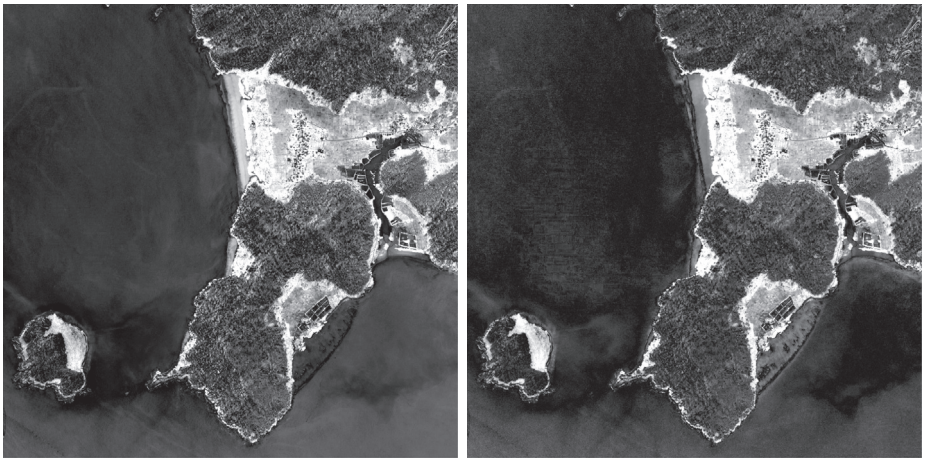

(c) Basic-SAM (d) NDVI

Fig. 8. Quickbird Case. Difference images (grayscale) obtained by the evaluated comparison methods.

For the proposed method the execution time increases, mainly due to the application of the SAM algorithm to each image independently. However, the runtime remains acceptable for real-time applications.

4. Conclusion

The proposed scheme offers an alternative that uses a typical spectral signature of vegetation as a reference spectrum for unsupervised change detection using the SAM index. The scheme has showed better results (overall accuracy and kappa index) than other unsupervised methods, particularly NDVI differencing and basic-SAM (without reference spectrum). These results were obtained by comparing the unsupervised methods against a supervised scheme based on post-classification SVM; in this sense, the results of the proposed method are similar to those given by the supervised scheme, supported by low detection of false positives and false negatives.

The proposed method was implemented in images of two different sensors. In the case of MS SPOT5 images, the Green, Blue and NIR bands were used for the definition of the reference spectrum. The result was an overall accuracy greater than 99% and a κ index greater than 90%. This indicates that the results of the method were able to identify most of the changes in vegetation present in an image with different soil types, as well as to avoid the detection of changed areas that did not correspond to vegetation. In the case of Quickbird images, the NIR band and the three bands in visible spectrum were used for the definition of the reference spectrum; also, the selected area presented natural disaster, with abundant changes in vegetation. The result was an accuracy greater than 97% and a κ index than 82%. It should be emphasized here that the dimensions of this image were superior to those of SPOT image, and that the radiometric resolution of this type of images is 11 bits. In any case, the results for the proposed method were better than the corresponding results for the methods implemented to detect changes in a specific land cover. The above corroborates that the main novelty of the proposed method consists in the detection of changes in a specific land cover type (vegetation) and that its results are similar to those given by a supervised scheme.

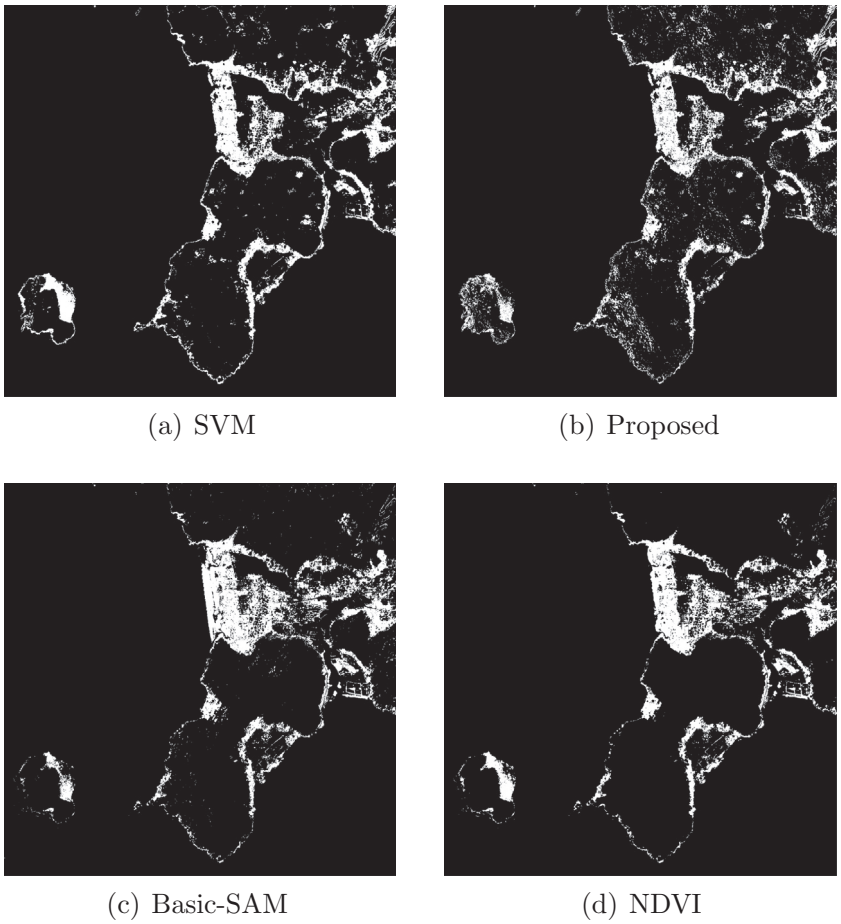

Fig. 9. Quickbird Case. CD masks obtained for the unsupervised detection methods and a supervised method (SVM-based). Change areas in white and non-change areas in black.

Table 2
Quickbird Case. Classification accuracy results obtained for the unsupervised detection methods, through the comparison against a supervised method (SVM-based) (results are shown in percentages).

Comparison and thresholding method		C	NC	Total	OA (%)	κ (%)
Proposed	C	142408	28347	170755	97.5	82.16
	NC	27896	2051349	2079245		
Basic-SAM	C	119153	36961	156114	96.08	70.90
	NC	51151	2042735	2093886		
NDVI	C	126046	22576	148622	97.03	77.45
	NC	44258	2057120	2101378		
	Total	170304	2079696	2250000		

C: Change (pixels) and NC: No-change (pixels).

Table 3
Execution times for the different evaluated unsupervised change detection methods.

Image	Proposed	NDVI	Basic-SAM
Spot (s)	0.5983	0.26934	0.7264
Quickbird (s)	2.4799	0.4099	1.6500

Another objective of the proposed method was the low computational load. In this sense, execution times were compared against unsupervised methods of low computational load. In this context, the main finding is that the precision results of the method are comparable to those of a supervised method, while the execution times are comparable to those of unsupervised methods of low computational load.

Finally, although these results are based on the use of limited data, further work is required such as the use of other types of coverage and the use of images with a higher number of spectral bands, as is the case of hyperspectral imagery.

References

Aggarwal, S., 2004. Principles of remote sensing. Satellite Rem. Sens. GIS Appl. Agric. Meteorol. 23.

Bovolo, F., Bruzzone, L., Marconcini, M., 2007. An unsupervised change detection technique based on bayesian initialization and semisupervised svm. In: 2007 IEEE International Geoscience and Remote Sensing Symposium. IEEE, pp. 2370–2373.

Bovolo, F., Camps-Valls, G., Bruzzone, L., 2010. A support vector domain method for change detection in multitemporal images. Pattern Recogn. Lett. 31 (10), 1148–1154.

Bovolo, F., Marchesi, S., Bruzzone, L., 2012. A framework for automatic and unsupervised detection of multiple changes in multitemporal images. IEEE Trans. Geosci. Rem. Sens. 50 (6), 2196–2212.

Carvalho Júnior, O.A., Guimarães, R.F., Gillespie, A.R., Silva, N.C., Gomes, R.A., 2011. A new approach to change vector analysis using distance and similarity measures. Rem. Sens. 3 (11), 2473–2493.

De Carvalho, O.A., Meneses, P.R., 2000. Spectral correlation mapper (scm): an improvement on the spectral angle mapper (sam). Summaries of the 9th JPL Airborne Earth Science Workshop, JPL Publication 00-18, vol. 9. JPL Publication, Pasadena, CA.

Foody, G.M., 2002. Status of land cover classification accuracy assessment. Rem. Sens. Environ. 80 (1), 185–201.

Im, J., Rhee, J., Jensen, J.R., Hodgson, M.E., 2007. An automated binary change detection model using a calibration approach. Rem. Sens. Environ. 106 (1), 89–105.

Kapur, J., Sahoo, P.K., Wong, A., 1985. A new method for gray-level picture thresholding using the entropy of the histogram. Comput. Vis. Graph. Image Process. 29 (3), 273–285.

Keshava, N., 2004. Distance metrics and band selection in hyperspectral processing with applications to material identification and spectral libraries. IEEE Trans. Geosci. Rem. Sens. 42 (7), 1552–1565.

Lu, D., Mausel, P., Brondizio, E., Moran, E., 2004. Change detection techniques. Int. J. Rem. Sens. 25 (12), 2365–2401.

Lu, D., Weng, Q., 2007. A survey of image classification methods and techniques for improving classification performance. Int. J. Rem. Sens. 28 (5), 823–870.

Martínez, E., Gonzalo, C., Arquero, A., Gordo, O., 1999. Evaluation of different fuzzy knowledge acquisition methods for remote sensing image classification. IEEE 1999 International Geoscience and Remote Sensing Symposium, 1999. IGARSS'99 Proceedings, vol. 5. IEEE, pp. 2489–2491.

Moughal, T.A., Yu, F., 2014. An automatic unsupervised method based on context-sensitive spectral angle mapper for change detection of remote sensing images. In: Advanced Data Mining and Applications. Springer, pp. 151–162.

Otsu, N., 1975. A threshold selection method from gray-level histograms. Automatica 11 (285–296), 23–27.

Rees, G., Rees, W.G., 2013. Physical Principles of Remote Sensing. Cambridge University Press.

Renza, D., Martinez, E., Arquero, A., 2011. Quality assessment by region in spot images fused by means dual-tree complex wavelet transform. Adv. Space Res. 48 (8), 1377–1391.

Renza, D., Martinez, E., Arquero, A., 2013. A new approach to change detection in multispectral images by means of ergas index. IEEE Geosci. Rem. Sens. Lett. 10 (1), 76–80.

Rosin, P., 1998. Thresholding for change detection. In: Sixth International Conference on Computer Vision, 1998. IEEE, pp. 274–279.

Rosin, P.L., Ioannidis, E., 2003. Evaluation of global image thresholding for change detection. Pattern Recogn. Lett. 24 (14), 2345–2356.

Sahoo, P.K., Soltani, S., Wong, A.K., 1988. A survey of thresholding techniques. Comput. Vis. Graph. Image Process. 41 (2), 233–260.

Sezgin, M., Sankur, B., 2004. Survey over image thresholding techniques and quantitative performance evaluation. J. Electron. Imag. 13, 146–165.

Shah-Hosseini, R., Homayouni, S., Safari, A., 2015a. Environmental monitoring based on automatic change detection from remotely sensed data: kernel-based approach. J. Appl. Rem. Sens. 9 (1), 095992–095992.

Shah-Hosseini, R., Homayouni, S., Safari, A., 2015b. A hybrid kernel-based change detection method for remotely sensed data in a similarity space. Rem. Sens. 7 (10), 12829–12858.

Singh, A., 1989. Review article digital change detection techniques using remotely-sensed data. Int. J. Rem. Sens. 10 (6), 989–1003.

Srivastava, P.K., Han, D., Rico-Ramirez, M.A., Bray, M., Islam, T., 2012. Selection of classification techniques for land use/land cover change investigation. Adv. Space Res. 50 (9), 1250–1265.

Teng, S., Chen, Y., Cheng, K., Lo, H., 2008. Hypothesis-test-based landcover change detection using multi-temporal satellite images – a comparative study. Adv. Space Res. 41 (11), 1744–1754.

Tewkesbury, A.P., Comber, A.J., Tate, N.J., Lamb, A., Fisher, P.F., 2015. A critical synthesis of remotely sensed optical image change detection techniques. Rem. Sens. Environ. 160, 1–14.

Tsai, W.-H., 1985. Moment-preserving thresolding: a new approach. Comput. Vis. Graph. Image Process. 29 (3), 377–393.

van der Meer, F., 2006. The effectiveness of spectral similarity measures for the analysis of hyperspectral imagery. Int. J. Appl. Earth Observ. Geoinform. 8 (1), 3–17.

Volpi, M., Tuia, D., Camps-Valls, G., Kanevski, M., 2010. Unsupervised change detection by kernel clustering. In: Remote Sensing. International Society for Optics and Photonics, 78300V–78300V.

Volpi, M., Tuia, D., Camps-Valls, G., Kanevski, M., 2012. Unsupervised change detection with kernels. IEEE Geosci. Rem. Sens. Lett. 9 (6), 1026–1030.

Wang, Y., Mitchell, B., Nugranad-Marzilli, J., Bonynge, G., Zhou, Y., Shriver, G., 2009. Remote sensing of land-cover change and landscape context of the national parks: a case study of the northeast temperate network. Rem. Sens. Environ. 113 (7), 1453–1461.

Weng, Q., Ehlers, M., Sofina, N., Filippovska, Y., Kada, M., 2014. Automated techniques for change detection using combined edge segment texture analysis, gis, and 3d information. In: Global Urban Monitoring and Assessment through Earth Observation. CRC Press, pp. 325–352.